Regionalization and morphological integration in the vertebral column of Eurasian small-bodied newts (Salamandridae: Lissotriton)

Aleksandar Urošević, Maja Ajduković, Tijana Vučić, Stefan J. Scholtes, Jan W. Arntzen, Ana Ivanović

DOI:
https://doi.org/10.1002/jez.b.23205

Received: 20 July 2022 | Revised: 30 March 2023 | Accepted: 11 May 2023

DOI: 10.1002/jez.b.23205

RESEARCH ARTICLE

JEZ-B MOLECULAR AND DEVELOPMENTAL EVOLUTION WILEY

Regionalization and morphological integration in the vertebral column of Eurasian small-bodied newts (Salamandridae: *Lissotriton*)

Aleksandar Urošević[1] | Maja Ajduković[1] | Tijana Vučić[2,3,4] | Stefan J. Scholtes[4] | Jan W. Arntzen[3,4] | Ana Ivanović[2]

[1]Department of Evolutionary Biology, Institute for Biological Research "Siniša Stanković," National Institute of the Republic of Serbia, University of Belgrade, Belgrade, Serbia

[2]Institute of Zoology, Faculty of Biology, University of Belgrade, Belgrade, Serbia

[3]Animal Sciences, Institute of Biology, Leiden University, Leiden, The Netherlands

[4]Naturalis Biodiversity Center, Leiden, The Netherland

Correspondence

Aleksandar Urošević, Department of Evolutionary Biology, Institute for Biological Research "Siniša Stanković," National Institute of the Republic of Serbia, University of Belgrade, Belgrade, Serbia.
Email: aurosevic@ibiss.bg.ac.rs

Funding information

Serbian Ministry of Education, Science and Technological Development grants numbers 451-03-68/2022-14/ 200007 and 451-03-68/2022-14/200178

Abstract

Serially homologous structures may have complex patterns of regionalization and morphological integration, influenced by developmental *Hox* gene expression and functional constraints. The vertebral column, consisting of a number of repeated, developmentally constrained, and highly integrated units—vertebrae—is such a complex serially homologous structure. Functional diversification increases regionalization and modularity of the vertebral column, particularly in mammals. For salamanders, three concepts of regionalization of the vertebral column have been proposed, recognizing one, two, or three presacral regions. Using three-dimensional geometric morphometrics on vertebra models acquired with microcomputerized tomography scanning, we explored the covariation of vertebrae in four closely related taxa of small-bodied newts in the genus *Lissotriton*. The data were analyzed by segmented linear regression to explore patterns of vertebral regionalization and by a two-block partial least squares method to test for morphological integration. All taxa show a morphological shift posterior to the fifth trunk vertebra, which corresponds to the two-region concept. However, morphological integration is found to be strongest in the mid-trunk. Taken jointly, these results indicate a highly integrated presacral vertebral column with a subtle two-region differentiation. The results are discussed in relation to specific functional requirements, developmental and phylogenetic constraints, and specific requirements posed by a biphasic life cycle and different locomotor modes (swimming vs. walking). Further research should be conducted on different ontogenetic stages and closely related but ecologically differentiated species.

KEYWORDS

axial skeleton, geometric morphometrics, micro-CT scanning, modularity, regional differentiation, serial homology, tailed amphibians

1 | INTRODUCTION

Morphological integration is defined as the covariation of morphological traits as a result of developmental and functional interactions (Olson & Miller, 1958), but may also be shaped by selective pressures (Cheverud, 1996; Klingenberg, 2008; Wagner & Altenberg, 1996; Zelditch & Goswami, 2021). Modularity implies variation in integration within an organism and some parts can be more integrated than others. Accordingly, morphological modules are interpreted as units with strong covariation within and minor covariation among units.

Serially homologous structures such as vertebrae, teeth, and ribs provide worthwhile model systems for the study of regionalization, modularity, and morphological integration, because they share a common structural plan with variation throughout the series (Gómez-Robles & Polly, 2012; Jones et al., 2018; Urošević et al., 2020). Elements within serially homologous structures tend to be developmentally constrained and strongly integrated (Asher et al., 2011; Carroll, 2001; Cowley & Atchley, 1990; Jones et al., 2018, 2020; Young & Hallgrímsson, 2005). In some cases, different functional demands and selection pressures may lead to the "parcellation" of regional differentiation (Wagner & Altenberg, 1996), such as in the limb skeleton (Young & Hallgrímsson, 2005), the feeding apparatus (Wainwright, 2007) and the vertebral column (Jones et al., 2020; Randau & Goswami, 2017). For example, the mammalian presacral vertebral column is markedly regionalized and can be divided into several developmental and functional modules (Randau & Goswami, 2017).

The evolution of vertebral modularity appears largely driven by locomotion and ecology (Galis et al., 2014; Jones et al., 2018) and is also under developmental constraints (Galis, 1999). The vertebral column can be viewed as an integrated structure because it derives entirely from the somites (the presomitic mesoderm) and it has independent developmental and evolutionary patterns derived from the abaxial domain of the mesoderm (Shearman & Burke, 2009). The shape of vertebrae and regionalization of the vertebral column are determined throughout the early ontogenetic stages by spatial and temporal expression of the *Hox* genes during somitogenesis (Aulehla & Pourquie, 2010; Krumlauf, 1994; Mallo et al., 2010). The boundaries in *Hox* genes expression correspond to the boundaries of the vertebral regions. In mammals, the expression boundary of the *Hox6* gene determines the cervicothoracic transition, *Hox*10 the thoraco-lumbar, and *Hox*11 the lumbar-sacral transition (Burke et al., 1995; Kuratani, 2009; Wellik, 2007). This tetrapod-like organization of *Hox* genes expression has presumably a deep evolutionary origin and may have arisen in the first jawed vertebrates (Criswell et al., 2021). Some well-preserved fossil skeletons of the early tetrapod *Ichthyostega* had recognizable thoracic, lumbar, sacral, and caudal vertebral regions (Ahlberg et al., 2005), suggesting that the regionalization of the vertebral column was, be it only subtly expressed, present in the stem tetrapod lineage (Head & Polly, 2015; Jones et al., 2018).

In extant amphibians, the vertebral column encompasses three distinctive body plans as found in the tailless frogs and toads (Anura), the elongated, limbless caecilians (Gymnophiona), and the tailed amphibians or salamanders (Caudata). Salamanders have a cylindrical body with a poorly differentiated vertebral column, four relatively short appendages and a tail (Duellman & Trueb, 1994; Mivart, 1870). They have widely been used as morphological analogs to the early terrestrial vertebrates that presumably possessed the same general body plan and similar modes of locomotion. Their presacral vertebral column consists of a single cervical vertebra (the atlas) which articulates to the skull and lack ribs, and a series of rib-bearing trunk vertebrae. They also have a single sacral vertebra, several postsacral, and numerous caudal vertebrae, depending on the species (Duellman & Trueb, 1994; Lanza et al., 2010; Litvinchuk & Borkin, 2003) (Figure 1a). Recent studies on vertebral regionalization (Jones et al., 2018) and morphological differentiation (Scholtes et al., 2021) indicate that the trunk region in salamanders is not as uniform as previously thought. A three-region pattern of the presacral vertebral column was found in *Ambystoma* (Jones et al., 2018). In small-bodied newts of the genus *Lissotriton* substantial morphological differentiation in the vertebrae shape along the trunk region was documented (Figure 1a; Scholtes et al., 2021). We here provide a brief description of three alternative concepts of the salamander's presacral vertebral column regionalization (see Table 1).

The vertebral column of tailed amphibians has traditionally been regarded as not, or poorly differentiated (Mivart, 1870; Duellman & Trueb, 1994; Slijepčević et al., 2015). The presacral vertebral column was in its entirety (minus the atlas) designated as the "trunk region", due to a shared gross morphology of rib-bearing vertebrae. Subsequently, Jones et al. (2018), using *Ambystoma* as model species, proposed a three-region differentiation of the salamander presacral vertebral column. The first region associates with the posterior branch of the brachial plexus, implying homology of the anterior trunk vertebrae with the cervical region, whereas the middle and posterior regions correspond to regions of short and long ribs in the Amniotes (Jones et al., 2018). Alternatively, studies on morphometric variation in vertebrae size (Govedarica et al., 2017; Worthington & Wake, 1972) and shape (Scholtes et al., 2021) revealed morphological differentiation (substantial disparity in size and shape) of the presacral vertebral column in salamanders, particularly in the anterior trunk vertebrae. A similar heterogeneity among short and bulky anterior and elongated posterior vertebrae was documented in caecilians (Lowie et al., 2022). The morphological differentiation and disparity of anterior trunk vertebrae have been explained by different functional demands upon anterior vertebrae compared to the subsequent, posterior ones (Scholtes et al., 2021; Worthington & Wake, 1972).

We gathered data on *Lissotriton* vertebrae size and shape to analyze patterns of covariation (allometric variation, regionalization, and integration), and we discuss our findings relative to three concepts of differentiation of the vertebral column in salamanders. Allometric variation is analyzed because it is generated by variation in developmental processes that affect multiple traits, resulting in overall patterns of covariation, and it contributes to morphological integration and modularity (Klingenberg, 2013; Mitteroecker & Bookstein, 2007; Hallgrímsson et al., 2019). To explore regionalization, we used segmented linear regression (SLR) (Head & Polly, 2015;

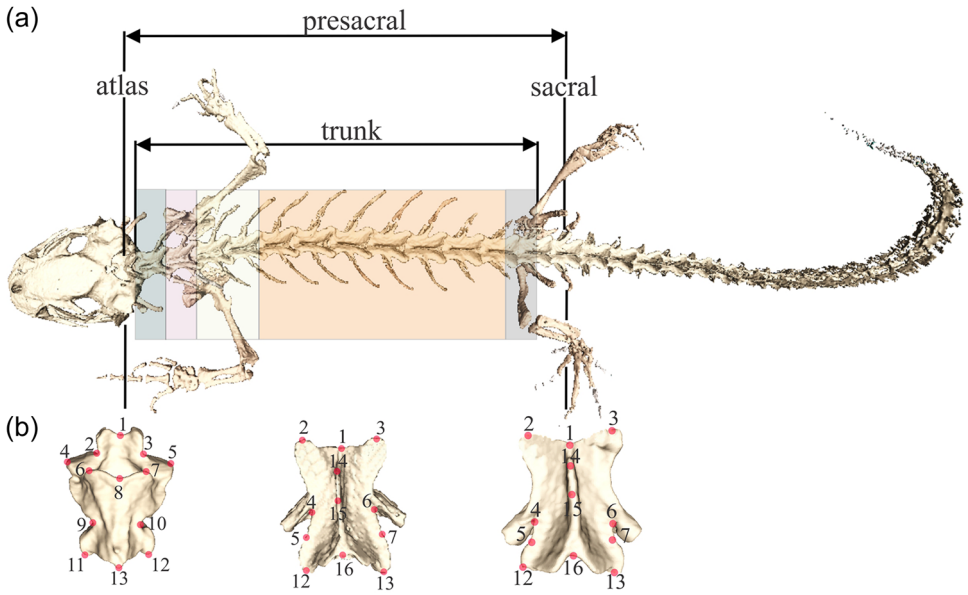

FIGURE 1 Morphological differentiation and regionalization of the presacral vertebral column in *Lissotriton* newts showing (a) different morphologies of trunk vertebrae, indicated by different color shadings, and (b) the configuration of the landmarks used to describe the shape of the atlas and the trunk and sacral vertebrae.

TABLE 1 Concepts of regional differentiation of the presacral vertebral column in tailed amphibians.

Concept 1	Traditional, one region
Regions recognized	Trunk
Source	Mivart (1870), Duellman and Trueb (1994), Slijepčević et al. (2015)
Concept 2	A three-region pattern conserved across the Tetrapods
Regions recognized	Cervical, anterior dorsal, and posterior dorsal
Source	Jones et al. (2018)
Concept 3	A two-region pattern based on morphological disparity and functional differentiation
Regions recognized	Anterior trunk and posterior trunk
Source	Worthington and Wake (1972), Govedarica et al. (2017), Scholtes et al. (2021), present study

Jones et al., 2018), which provides information on the most probable changes in the pattern of covariation and suggests possible regions. Morphological integration was quantified as the strength of covariation among vertebrae using two-block partial least squares (PLS) (e.g., Bastir & Rosas, 2005; Klingenberg, 2009). We expected to observe higher integration within regions and lower integration among vertebrae from different regions.

2 | RESULTS

2.1 | Analyses of allometric variation

The MANCOVA analysis testing for homogeneity of allometric slopes between sub(species) over individual vertebrae (Supporting Information: Table S3) showed that allometry was not statistically significant, except for the 10th and 11th trunk vertebrae ($F_{26,42} = 2.85$, $p = 0.0012$ and $F_{26,39} = 3.06$, $p = 0.0008$, respectively). A significant (sub) species × logCS interaction ($F_{78,117.49} = 1.87$, $p = 0.001$) was found only for the seventh trunk vertebra, which also diverged in shape among taxa ($F_{78,117.49} = 1.81$, $p = 0.002$).

A statistically significant difference of allometric slopes of vertebrae was found within the vertebral column (Table 2). Pairwise comparisons revealed highly significant slope differences between the 3rd and 5th, as well as and 6th and 12th trunk vertebrae (Table 3). Because of the absence of statistically significant allometry at the sub(species) level and statistically significant differences in allometric slopes between vertebrae along the vertebral column, we did not apply a correction for allometry in subsequent analyses.

2.2 | Trunk regionalization

Similar patterns of variation in vertebrae shape were found across the four (sub)species (Figure 2). In all taxa, the first and second PC axes together explained >90% of the total shape variation. The first axis explained a shape gradient from the shortened and widened anterior vertebrae with increased height to the elongated, narrower posterior vertebrae with reduced height. The second axis explained a shift from the mid-trunk vertebrae which were shorter, with a higher neural arch to the posterior-most vertebrae that were elongated, with a reduced neural arch (Figure 2). The SLR analyses yielded the best fit for the two-region model (Table 1). The transition point corresponded to the fifth trunk vertebra in all taxa (Table 4, Figure 3).

2.3 | Morphological integration

The estimation of morphological integration ranged from moderate (0.3 < RV < 0.5) to strong (RV > 0.5) and was statistically significant for all pairs of vertebrae, except for the atlas and all other vertebrae, excluding the first, second, and fifth trunk vertebrae. The strongest morphological integration was detected at the sixth and seventh trunk vertebrae (Figure 4; Supporting Information: Table S2). Integration levels estimated from *z* scores vary from weak ($z < 2$) to moderate ($2 < z < 4$) and strong ($z > 4$) and were the highest between the third and seventh trunk vertebrae. The strongest integration between adjacent vertebrae was between the first and second, second and third, fifth and sixth, and eighth and ninth trunk vertebrae. Among the adjacent trunk vertebrae, there was no significant integration between the 9th and 10th and the 11th and 12th (Figure 4, Supporting Information: Table S4).

TABLE 2 Homogeneity of slopes in *Lissotriton v. vulgaris*, with the effect of vertebrae, size (logCS), and vertebra × logCS interaction, tested by a multivariate analysis of covariance.

Effect	Wilks' λ	*F*	Effect *df*	Error *df*	*p*
Vertebra	0.836	1.74	55	2429.06	0.0007
LogCS	0.524	95.26	5	524.00	<0.0001
Vertebra × logCS	0.837	1.73	55	2429.06	0.0008

Note: Statistically significant interaction indicates heterogeneous regression slopes.

3 | DISCUSSION

The tetrapod body plan is determined by *Hox* genes and is largely developmentally constrained. The regionalization of the vertebral column in tetrapods, which is most pronounced in mammals, is largely driven by various functional demands (Carroll, 1997; Jones et al., 2018). Based on morphological, developmental, and functional criteria and the literature, we considered three concepts of vertebral column regionalization in salamanders, in which one, two, or three presacral regions are recognized (Table 1). Considering the results for both analytical methods separately, our data support the traditional concept of regionalization with a single, highly integrated trunk, and the two-region concept, which recognizes an anterior and a posterior trunk region.

The results are not unequivocal because the differentiation into an anterior and a posterior region with a break between the fifth and sixth trunk vertebrae recognized by the SLR analysis is not supported by the pattern of morphological integration observed by the PLS analysis. The vertebrae within regions should, by definition, be more integrated than between regions (Klingenberg, 2008; Wagner & Altenberg, 1996). However, the morphological integration is found to

TABLE 3 Results of MANCOVA tests for differences in allometric slopes among vertebrae.

	1	2	3	4	5	6	7	8	9	10	11
2	0.892										
3	0.852	0.981									
4	0.845	0.915	0.865								
5	0.828	0.829	**0.713**	0.961							
6	0.906	0.888	0.842	0.931	0.932						
7	0.871	0.899	0.803	0.968	0.965	0.949					
8	0.846	0.966	0.953	0.936	0.833	0.919	0.868				
9	0.910	0.933	0.892	0.961	0.960	0.975	0.974	0.952			
10	0.928	0.984	0.944	0.925	0.841	0.927	0.904	0.954	0.951		
11	0.874	0.975	0.957	0.963	0.869	0.912	0.888	0.984	0.946	0.966	
12	0.873	0.933	0.883	0.848	0.798	**0.775**	0.808	0.875	0.836	0.925	0.907

Note: Vertebrae are numbered from 1 to 12. Wilk's λ values in boldface type denote statistical significance for pairwise comparisons at $p < 0.05$ after Bonferroni correction, with an adjusted α value of 0.0008.

Abbreviation: MANCOVA, multivariate analysis of covariance.

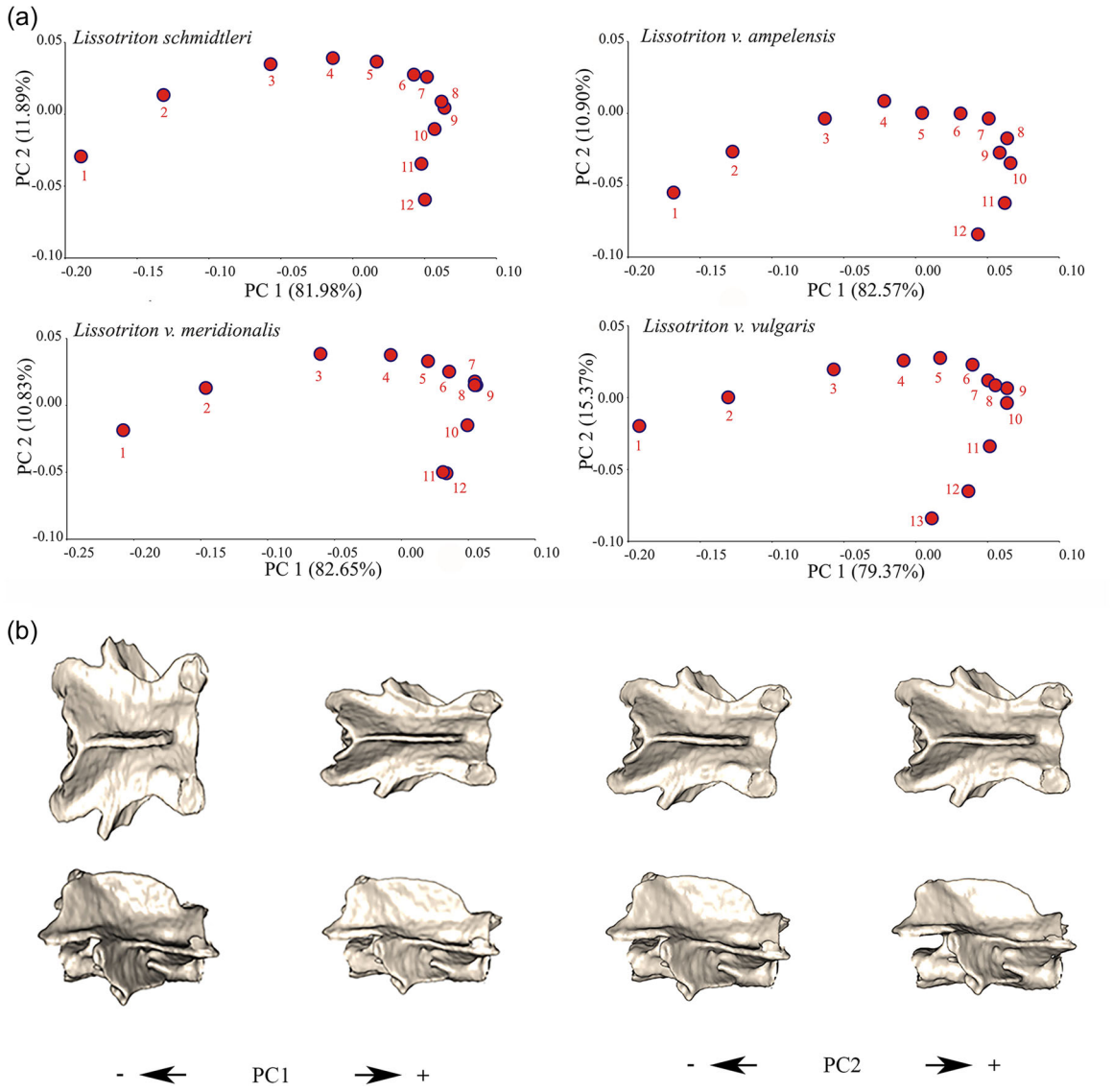

FIGURE 2 Shape changes of trunk vertebrae in four *Lissotriton* taxa with (a) the position of the trunk vertebrae over numbers 1–12 or 13, and (b) the gradient of shape changes over the first and second principal component axis.

be strongest in the mid-trunk (Figure 4), where the breakpoint between the regions is detected (Figure 3). The strong individual integration between the adjacent first, second, and third vertebrae could be related to the center of the anterior region, whereas the atlas, sacral vertebra, and 12th trunk vertebra tend to have some autonomy from the remaining trunk vertebrae.

In summary, our results suggest a subtle pattern of regionalization, corresponding to a functionally based, two-region concept, despite a high level of integration that was observed in the anterior and middle parts of the presacral vertebral column. The marked morphological integration could be explained by the homogeneity of the whole vertebral column as possibly required for its functional stability (Arlegi et al., 2020). In salamanders, the vertebral column, together with the axial musculature, provides support and locomotion in aquatic as well as terrestrial environments (Duellman & Trueb, 1994). The axial musculoskeletal system in salamanders has been described in detail for the fire salamander, *Salamandra salamandra* (Linnaeus, 1758) (Francis, 1934). The dorsal musculature arrangement is more or less uniform, with a main function in the bending and flexion of the spine. The first to fifth trunk vertebrae are involved in movements of the pectoral girdle and the front limbs. The first and second trunk vertebrae are connected with the cranial skeleton with the muscles involved in the coordinated head movement and spine flection (Francis, 1934). This could explain the covariation between the first to fifth trunk vertebrae, notwithstanding their differences in shape (Scholtes et al., 2021). The posterior region (from the 6th to the 11th or the 12th vertebra) consists of vertebrae with similar shape and the same arrangement of muscles driving the lateral bending of the trunk during swimming and walking.

In salamanders, the axial skeleton forms during early development and remains largely unchanged during the metamorphosis. It has been proposed that the complex life cycle, with opposing functional

TABLE 4 Results of a segmented linear regression analysis on vertebrae shape averaged for *Lissotriton* (sub)species.

(Sub)species	Regions	T1	T2	sumRSS	AICc	ΔAIC	model_lik	Ak_weight
Lissotriton schmidtleri	**2**	**5**	**0**	**2.75**	**−21.19**	**0.00**	**1.0000**	**0.9937**
	3	3	5	0.68	−10.92	10.26	0.0059	0.0059
	1	0	0	12.35	−5.85	15.34	0.0005	0.0005
Lissotriton v. ampelensis	**2**	**5**	**0**	**3.02**	**−18.86**	**0.00**	**1.0000**	**0.8253**
	3	4	7	0.55	−15.74	3.12	0.2102	0.1735
	1	0	0	12.35	−5.84	13.03	0.0015	0.0012
Lissotriton v. meridionalis	**2**	**5**	**0**	**2.28**	**−25.61**	**0.00**	**1.0000**	**0.9998**
	3	3	9	0.78	−7.71	17.90	0.0001	0.0001
	1	0	0	11.91	−6.71	18.89	0.0001	0.0001
Lissotriton v. vulgaris	**2**	**5**	**0**	**1.81**	**−40.06**	**0.00**	**1.0000**	**0.9654**
	3	4	9	0.56	−33.40	6.66	0.0359	0.0346
	1	0	0	12.99	−8.14	31.93	0.0000	0.0000

Note: The most likely regionalization models are shown in boldface type.

Abbreviations: AICc, Akaike information criterion adjusted for small sample size; Ak_weight, Akaike weight; ml, model likelihood; Regions, number of regions in the model; sumRSS, residual sum of squares; T1 and T2, transition points 1 and 2; ΔAIC, change in AIC score from one model to the next.

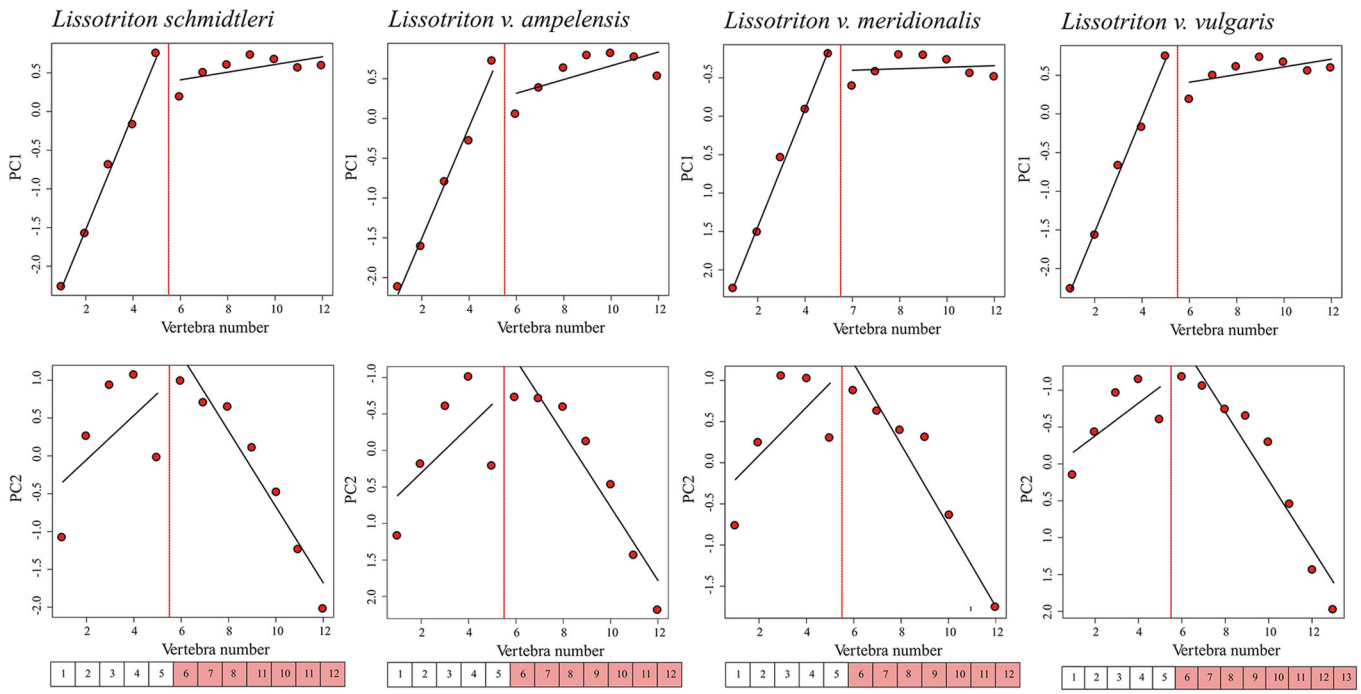

FIGURE 3 Results of segmented linear regression analysis of the trunk vertebrae in four *Lissotriton* taxa. Dots show the scores along the first (top panel) and second (bottom panel) axis of a principal component analysis for vertebrae 1–12. Region models are shown in bars below each of the graphs.

requirements upon the axial skeleton during the larval and adult phases, constrains evolutionary changes in the vertebral column (Bonett & Blair, 2017). Therefore, changes in the pattern of regionalization might be expected in nonmetamorphic taxa, including paedomorphic lineages (e.g., Sirenidae, Proteidae) and in lineages with direct development (Plethodontidae). However, a different regionalization pattern was found in *Ambystoma* with three regions (Jones et al., 2018) and *Lissotriton* with two regions (this study), that both have a complex life cycle and similar requirements for locomotory performance (swimming vs. walking). Compared to the three-region concept of differentiation described for *Ambystoma* (Jones et al., 2018), the anterior trunk region in *Lissotriton* coincides with the "cervical" region, whereas the posterior

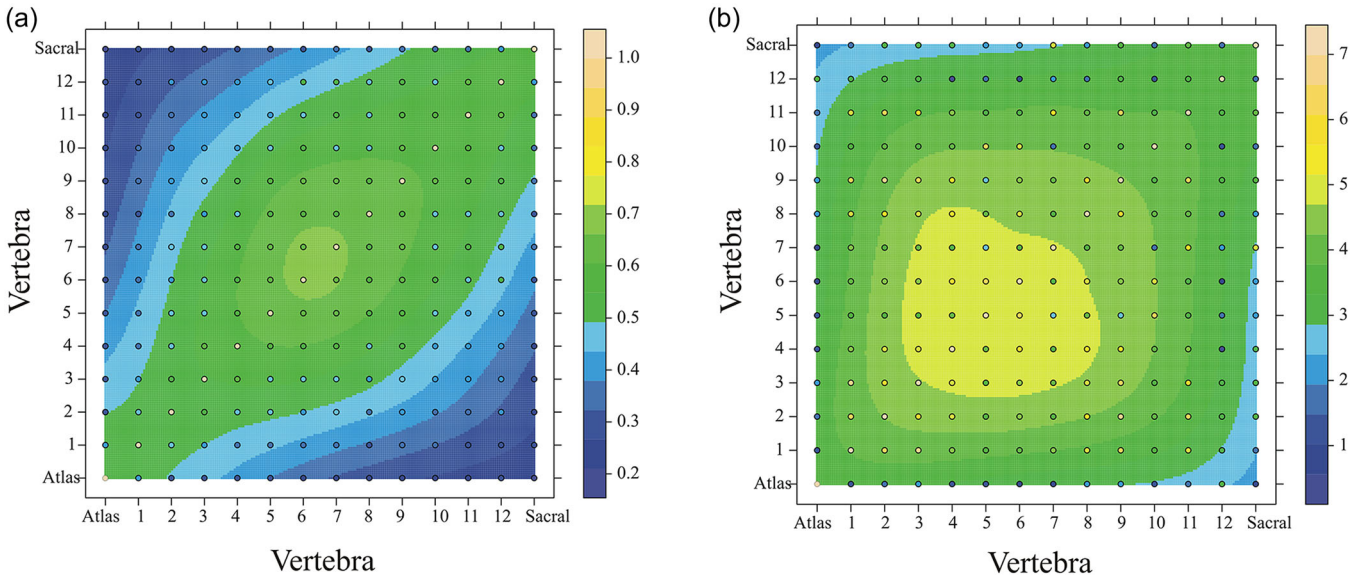

FIGURE 4 Heat maps presenting patterns of morphological integration of the presacral vertebral column in *Lissotriton* newts. Dots represent individual pairwise correlations corrected for (sub)species for (a) RV scores on the symmetric component of the shape variation and (b) *z* scores on total shape. For actual values, see color bars.

trunk region is uniform, without detectable differentiation in the subsequent anterior and posterior "dorsal" region (Jones et al., 2018). As the clades *Ambystoma* and *Lissotriton* are unrelated, it is possible that *Ambystoma* kept the ancestral condition of regionalization including an ancestral amphicoelous morphology of the vertebrae, compared to the derived condition of ophisthocoelous vertebrae found in the family Salamandridae (Duellman & Trueb, 1994; Worthington & Wake, 1972). The morphometric study of Worthington and Wake (1972) also found that species belonging to different lineages of tailed amphibians (namely Ambystomatidae, Salamandridae, and Plethodontidae) have different patterns of morphometric variation along the vertebral column.

To further explore patterns of vertebral regionalization, modularity, and morphological integration in salamanders, it would be beneficial to include different life stages (e.g., larvae vs. metamorphs), or closely related, but ecologically differentiated forms. For the genus *Lissotriton*, this points to paedomorphic populations such as found in *L. vulgaris* (Toli et al., 2022) and to the frequently stream-dwelling *L. boscai* (Tourneville, 1879) from the Iberian Peninsula. Related species with different numbers of presacral vertebrae such as found within the genera *Triturus* and *Tylototriton* warrant attention (Arntzen et al., 2015), as does the genus *Salamandra* for which larviparous, pueriparous, and viviparous lineages can be compared (Buckley et al., 2007). Ideally, these studies would be accompanied by data on *Hox* gene expression.

4 | MATERIALS AND METHODS

The studied material consists of 74 adult male specimens belonging to two closely related species *Lissotriton schmidtleri* (Raxworthy, 1988) and *L. vulgaris*, the latter being represented by the subspecies *L. v. vulgaris* (Linnaeus, 1758), *L. v. ampelensis* (Fuhn, 1951), and *L. v. meridionalis* (Boulenger, 1882). These taxa were chosen because they are phylogenetically close (Pabijan et al., 2017) and show similar patterns of morphological differentiation of the trunk region (Scholtes et al., 2021).

The material was either ethanol preserved as is, or prepared as cleared and stained skeletons preserved in glycerin. Detailed sample data on taxonomy, geographical origin, type of preservation, and collection details are provided in Appendix A. For each specimen, the atlas, the 1st–12th or 13th trunk vertebrae and the sacral vertebrae were scanned with a SkyScan 1172 microcomputerized tomography scanner (Bruker Corporation) at a resolution of 26.33 µM (32 kV, 0.5 µM aluminum filter, 0.7° rotation steps, 175 ms exposure time, 180° object scanning and a manual flat field correction set at 35 kV). The data were processed into 3D models with Avizo 9.5 software (FEI; Thermo Fisher Scientific) (Figure 1a). The configurations of 14 landmarks for the atlas and 18 landmarks for the trunk and sacral vertebrae (Figure 1b) were digitized using the Landmark IDAV 141 v.3.6 software (https://landmark2.software.informer.com/3.6/) by a single observer (M. A.). A morphological description of the landmarks is provided in Appendix B. Raw morphometric data are provided in Supporting Information: Data S1.

4.1 | Shape variables

We generated the matrix of shape coordinates for each vertebra using a generalized Procrustes analysis (GPA) (Dryden & Mardia, 1998; Rohlf & Slice, 1990), that accounts for object symmetry and quantifies the symmetric components of shape variation (Klingenberg et al., 2002). The principal components (PC scores) from principal component analysis were used as shape variables and centroid size (CS) was used as a measure of

general size (Zelditch et al., 2012). CS values are provided in Supporting Information: Data S1). For the subset of individuals ($N = 12$, 7 *L. v. meridionalis* and 5 *L. v. vulgaris*) for which standard length (snout-vent length, SVL) was available, we found a strong correlation between CS and standard body length ($r = 0.88$, $p < 0.05$, and $r = 0.99$, $p < 0.05$, respectively).

4.2 | Analyses of allometric variation

For each vertebra, the divergence in allometric slopes among taxa was tested for homogeneity of regression slopes with a multivariate analysis of covariance (MANCOVA), with shape variables (PC scores) as the dependent variables, (sub)species as a factor and log-transformed CS (logCS) as a covariate. For the comparisons of allometric variation among vertebrae within the vertebral column, the subset of *T. v. vulgaris* with the largest sample size ($N = 47$, Appendix I) was used. The homogeneity of slopes was similarly tested with vertebra as a factor. The differences in allometric slopes between vertebrae were further explored by comparisons of allometric regression slopes among vertebrae. At statistical evaluation, the Bonferroni correction for multiple comparisons was applied. The PCAs were done with MorphoJ software v. 1.06 (Klingenberg, 2011) and MANCOVAs were done with the Statistica 10 software package (Statistica for Windows; StatSoft, Inc.).

4.3 | Trunk regionalization

Principal component analysis on the mean shape values of the individual trunk vertebrae for each (sub)species was used to explore patterns of shape variation and for SLR analyses. The series of continuous regression lines were fit to the slopes of the PC scores, and boundaries of regions were determined from the transition points that minimized the sum of squares (Head & Polly, 2015). The Akaike information criterion (AIC) weighted average of the relative fit was calculated to represent the amount of regionalization for each of the region models (Jones et al., 2018) with a maximum of three, for the cervical, thoracic, and lumbar region. The SLR- and AIC-fittings were calculated with the *Regions* package (Jones, 2018) in R version 4.1.1. (R Core Team, 2021).

4.4 | Morphological integration

To estimate the strength of covariation between vertebrae, we employed a two-block PLS analysis, based on a singular value decomposition of the matrix of covariances between the two sets of variables (Bookstein, 1991; Rohlf & Corti, 2000; Young & Hallgrímsson, 2005). This approach is suitable for testing covariation between the two separate sets of landmarks, with separate Procrustes superimpositions (Bastir & Rosas, 2005; Klingenberg, 2009; McCane & Kean, 2011; Neaux et al., 2013; Urošević et al., 2020). The measures of covariation between the vertebrae were the RV coefficient (Klingenberg, 2009, 2011) and *z* scores (Adams & Collyer, 2016). The RV coefficient is a generalization of Pearson's correlation coefficient (Escoufier, 1973). Statistical significance of the RV coefficients was assessed via a permutation test against a null hypothesis of total independence (Good, 2000; Klingenberg, 2009, 2011; Manly, 2007) under Bonferroni correction for multiple comparisons. Because the use of the RV coefficient has been criticized on the ground that it is sensitive to sample size and other variables (Adams, 2016; Adams & Collyer, 2016), we repeated analyses corrected for the effect of (sub) species by applying multivariate regression, with shape as the dependent variable and (sub)species numerically coded and used as an independent variable. Two-block PLS was then done on the regression residuals. For the quantification of the covariation strength, we used *z* scores, centred on their estimated empirically expected values, with statistical significance estimated by a randomization test with 999 permutations (Adams & Collyer, 2016).

Morphological integration was tested between structures (atlas, trunk, and sacral vertebrae) in pairwise manner on the covariance matrices pooled within taxa. RV coefficients were calculated with MorphoJ software v. 1.06 (Klingenberg, 2011) and *z* scores were calculated with *Geomorph 4.0.0*. package (Adams et al., 2021). A heat map visualization of the results was produced with the *Lattice* and *LatticeExtra* packages (Sarkar, 2008; Sarkar & Andrews, 2019) in R. All R scripts used are provided as Supporting Information: Data S2.

ACKNOWLEDGMENTS

We thank Katrina E. Jones for help and advice with the *Regions* package. We also thank two anonymous reviewers for critical comments and suggestions that helped to improve the manuscript. Our work was funded by the Serbian Ministry of Education, Science and Technological Development grants numbers 451-03-68/2022-14/200007 and 451-03-68/2022-14/200178.

CONFLICT OF INTEREST STATEMENT

The authors declare no conflict of interest.

DATA AVAILABILITY STATEMENT

The data are available as a supplementary file provided in the manuscript (Supporting Information: Data S1). The raw shape coordinates, size values (centroid size), and R scripts underlying this article are publicly available as Supporting Information: to the published version of the article.

ORCID

Aleksandar Urošević http://orcid.org/0000-0003-1158-5537
Maja Ajduković http://orcid.org/0000-0001-9115-6622
Tijana Vučić http://orcid.org/0000-0002-8850-5251
Stefan J. Scholtes http://orcid.org/0000-0001-9320-4296
Jan W. Arntzen http://orcid.org/0000-0003-3229-5993
Ana Ivanović http://orcid.org/0000-0002-6247-8849

PEER REVIEW

The peer review history for this article is available at https://www.webofscience.com/api/gateway/wos/peer-review/10.1002/jez.b.23205.

REFERENCES

Adams, D. C. (2016). Evaluating modularity in morphometric data: Challenges with the RV coefficient and a new test measure. *Methods in Ecology and Evolution*, *7*, 565–572. https://doi.org/10.1111/2041-210X.12511

Adams, D. C., & Collyer, M. L. (2016). On the comparison of the strength of morphological integration across morphometric datasets. *Evolution*, *70*, 2623–2631. https://doi.org/10.1111/evo.13045

Adams, D. C., Collyer, M. L., Kaliontzopoulou, A., & Baken, E. (2021). *Geomorph. Geometric morphometric analyses of 2D/3D landmark data*. R package. https://github.com/geomorphR/geomorph

Ahlberg, P. E., Clack, J. A., & Blom, H. (2005). The axial skeleton of the Devonian tetrapod *Ichthyostega*. *Nature*, *437*, 137–140. https://doi.org/10.1038/nature03893

Arlegi, M., Veschambre-Couture, C., & Gómez-Olivencia, A. (2020). Evolutionary selection and morphological integration in the vertebral column of modern humans. *American Journal of Physical Anthropology*, *171*, 17–36. https://doi.org/10.1002/ajpa.23950

Arntzen, J. W., Beukema, W., Galis, F., & Ivanović, A. (2015). Vertebral number is highly evolvable in salamanders and newts (family Salamandridae) and variably associated with climatic parameters. *Contributions to Zoology*, *84*, 85–113. https://doi.org/10.1163/18759866-08402001

Asher, R. J., Lin, K. H., Kardjilov, N., & Hautier, L. (2011). Variability and constraint in the mammalian vertebral column. *Journal of Evolutionary Biology*, *24*, 1080–1090. https://doi.org/10.1111/j.1420-9101.2011.02240.x

Aulehla, A., & Pourquie, O. (2010). Signaling gradients during paraxial mesoderm development. *Cold Spring Harbor Perspectives in Biology*, *2*, a000869. https://doi.org/10.1101/cshperspect.a000869

Bastir, M., & Rosas, A. (2005). Hierarchical nature of morphological integration and modularity in the human posterior face. *American Journal of Physical Anthropology*, *128*, 26–34. https://doi.org/10.1101/10.1002/ajpa.20191

Bonett, R. M., & Blair, A. L. (2017). Evidence for complex life cycle constraints on salamander body form diversification. *Proceedings of the National Academy of Sciences*, *114*, 9936–9941. https://doi.org/10.1073/pnas.1703877114

Bookstein, F. L. (1991). *Morphometric tools for landmark data: Geometry and biology*. Cambridge University Press.

Boulenger, G. A. 1882). Catalogue of the Batrachia Gradientia s.Caudata and Batrachia Apoda in the Collection of the British Museum. Second Edition. Taylor and Francis.

Buckley, D., Alcobendas, M., García-París, M., & Wake, M. H. (2007). Heterochrony, cannibalism, and the evolution of viviparity in *Salamandra salamandra*. *Evolution & Development*, *9*, 105–115. https://doi.org/10.1111/j.1525-142X.2006.00141.x

Burke, A. C., Nelson, C. E., Morgan, B. A., & Tabin, C. (1995). *Hox* genes and the evolution of vertebrate axial morphology. *Development*, *121*, 333–346. https://doi.org/10.1242/dev.121.2.333

Carroll, R. L. (1997). *Patterns and processes of vertebrate evolution*. Cambridge University Press.

Carroll, S.B. (2001). Chance and necessity: The evolution of morphological complexity and diversity. *Nature*, *409*, 1102–1109. https://doi.org/10.1038/35059227

Cheverud, J. M. (1996). Developmental integration and the evolution of pleiotropy. *American Zoologist*, *36*, 44–50.

Cowley, D. E., & Atchley, W. R. (1990). Development and quantitative genetics of correlation structure among body parts of *Drosophila melanogaster*. *The American Naturalist*, *135*, 242–268. https://doi.org/10.1086/285041

Criswell, K. E., Roberts, L. E., Koo, E. T., Head, J. J., & Gillis, J. A. (2021). *Hox* gene expression predicts tetrapod-like axial regionalization in the skate, *Leucoraja erinacea*. *Proceedings of the National Academy of Sciences*, *118*, e2114563118. https://doi.org/10.1073/pnas.2114563118

Dryden, I. L., & Mardia, K. V. (1998). *Statistical shape analysis*. Wiley.

Duellman, W. E., & Trueb, L. (1994). *Biology of amphibians*. Johns Hopkins University Press.

Escoufier, Y. (1973). Le traitement des variables vectorielles. *Biometrics*, *29*, 751–760. https://doi.org/10.2307/2529140

Francis, E. B. T. (1934). *The anatomy of the salamander*. Clarendon Press.

Fuhn, I. E. (1951). Contributiuni la sistematics Salamazdrelor din Republica Populara Romana. I. Studiul catorva populatii de *Triturus vulgaris* L. Buletinul Stiintific. Sectiunea deStiinte Biologice, Agronomice, Geologice si Geografice. Bucuresti, *3*, 501.

Galis, F. (1999). Why do almost all mammals have seven cervical vertebrae? Developmental constraints, *Hox* genes and cancer. *Journal of Experimental Zoology*, *285*, 19–26.

Galis, F., Carrier, D. R., van Alphen, J., van der Mije, S. D., Van Dooren, T. J. M., Metz, J. A. J., & ten Broek, C. M. A. (2014). Fast running restricts evolutionary change of the vertebral column in mammals. *Proceedings of the National Academy of Sciences*, *111*, 11401–11406. https://doi.org/10.1073/pnas.1401392111

Gómez-Robles, A., & Polly, P. D. (2012). Morphological integration in the hominin dentition: Evolutionary, developmental, and functional factors. *Evolution*, *66*, 1024–1043. https://doi.org/10.1111/j.1558-5646.2011.01508.x

Good, P. (2000). *Permutation tests: A practical guide to resampling methods for testing hypotheses* (2nd ed.). Springer.

Govedarica, P., Cvijanović, M., Slijepčević, M., & Ivanović, A. (2017). Trunk elongation and ontogenetic changes in the axial skeleton of *Triturus* newts. *Journal of Morphology*, *278*, 1577–1585. https://doi.org/10.1002/jmor.20733

Hallgrímsson, B., Katz, D. C., Aponte, J. D., Larson, J. R., Devine, J., Gonzalez, P. N., Young, N. M., Roseman, C. C., & Marcucio, R. S. (2019). Integration and the developmental genetics of allometry. *Integrative and comparative biology*, *59*, 1369–1381. https://doi.org/10.1093/icb/icz105

Head, J. J., & Polly, P. D. (2015). Evolution of the snake body form reveals homoplasy in amniote *Hox* gene function. *Nature*, *520*, 86–89. https://doi.org/10.1038/nature14042

Jones, K. E. (2018). *Regions. Find regions in serially-homologous structures*. R package. https://github.com/katrinajones/regions

Jones, K. E., Angielczyk, K. D., Polly, P. D., Head, J. J., Fernandez, V., Lungmus, J. K., Tulga, S., & Pierce, S. E. (2018). Fossils reveal the complex evolutionary history of the mammalian regionalized spine. *Science*, *361*, 1249–1252. https://doi.org/10.1126/science.aar3126

Jones, K. E., Gonzalez, S., Angielczyk, K. D., & Pierce, S. E. (2020). Regionalization of the axial skeleton predates functional adaptation in the forerunners of mammals. *Nature Ecology & Evolution*, *4*, 470–478. https://doi.org/10.1038/s41559-020-1094-9

Klingenberg, C. P. (2008). Morphological integration and developmental modularity. *Annual Review of Ecology, Evolution and Systematics*, *39*, 115–132. https://doi.org/10.1146/annurev.ecolsys.37.091305.110054

Klingenberg, C. P. (2009). Morphometric integration and modularity in configurations of landmarks: Tools for evaluating a-priori hypotheses. *Evolution & Development*, *11*, 405–421. https://doi.org/10.1111/j.1525-142X.2009.00347.x

Klingenberg, C. P. (2011). MorphoJ: An integrated software package for geometric morphometrics. *Molecular Ecology Resources*, *11*, 353–357. https://doi.org/10.1111/j.1755-0998.2010.02924.x

Klingenberg, C. P. (2013). Cranial integration and modularity: Insights into evolution and development from morphometric data. *Hystrix*, *24*, 43–58. https://doi.org/10.4404/hystrix-24.1-6367

Klingenberg, C. P., Barluenga, M., Meyer, A., Klingenberg, C. P., Barluenga, M., & Meyer, A. (2002). Shape analysis of symmetric structures: Quantifying variation among individuals and asymmetry. *Evolution*, *56*, 1909–1920.

Krumlauf, R. (1994). *Hox* genes in vertebrate development. *Cell*, *78*, 191–201. https://doi.org/10.1111/j.0014-3820.2002.tb00117.x

Kuratani, S. (2009). Modularity, comparative embryology and evo-devo: Developmental dissection of evolving body plans. *Developmental Biology*, *332*, 61–69. https://doi.org/10.1016/j.ydbio.2009.05.564

Lanza, B., Arntzen, J. W., & Gentile, E. (2010). Vertebral numbers in the Caudata of the Western Palaeartic (Amphibia). *Atti del Museo Civico di Storia Naturale di Trieste*, *54*, 3–114.

Linnaeus, C. (1758). *Systema naturae per regna tria naturae, secundum classes, ordines, genera, species, cumcharacteribus, differentiis, synonymis, locis. Tomus I*. Holmiæ. (Salvius).

Litvinchuk, S. N., & Borkin, L. J. (2003). Variation in number of trunk vertebrae and in count of costal grooves in salamanders of the family Hynobiidae. *Contributions to Zoology*, *72*, 195–209. https://doi.org/10.1163/18759866-07204001

Lowie, A., De Kegel, B., Wilkinson, M., Measey, J., O'Reilly, J. C., Kley, N. J., Gaucher, P., Brecko, J., Kleinteich, T., Herrel, A., & Adriaens, D. (2022). Regional differences in vertebral shape along the axial skeleton in caecilians (Amphibia: Gymnophiona. *Journal of Anatomy*, *241*, 716–728. https://doi.org/10.1111/joa.13682

Mallo, M., Wellik, D. M., & Deschamps, J. (2010). *Hox* genes and regional patterning of the vertebrate body plan. *Developmental Biology*, *344*, 7–15. https://doi.org/10.1016/j.ydbio.2010.04.024

Manly, B. F. J. (2007). *Randomization, bootstrap and Monte Carlo methods in biology*. Chapman & Hall/CRC.

McCane, B., & Kean, M. R. (2011). Integration of parts in the facial skeleton and cervical vertebrae. *American Journal of Orthodontics and Dentofacial Orthopedics*, *139*, e13–e30. https://doi.org/10.1016/j.ajodo.2010.06.016

Mitteroecker, P., & Bookstein, F. (2007). The conceptual and statistical relationship between modularity and morphological integration. *Systematic Biology*, *56*, 818–836. https://doi.org/10.1080/10635150701648029

Mivart, G. (1870). On the axial skeleton of the Urodela. *Proceedings of the Zoological Society of London*, *1870*, 260–278.

Neaux, D., Guy, F., Gilissen, E., Coudyzer, W., & Ducrocq, S. (2013). Covariation between midline cranial base, lateral basicranium, and face in modern humans and chimpanzees: A 3D geometric morphometric analysis. *The Anatomical Record*, *296*, 568–579. https://doi.org/10.1002/ar.22654

Olson, E. C., & Miller, R. L. (1958). *Morphological integration*. University of Chicago Press.

Pabijan, M., Zieliński, P., Dudek, K., Stuglik, M., & Babik, W. (2017). Isolation and gene flow in a speciation continuum in newts. *Molecular Phylogenetics and Evolution*, *116*, 1–12. https://doi.org/10.1016/j.ympev.2017.08.003

R Core Team. (2021). *R: A language and environment for statistical computing*. R Foundation for Statistical Computing. https://www.R-project.org/

Randau, M., & Goswami, A. (2017). Morphological modularity in the vertebral column of Felidae (Mammalia, Carnivora). *BMC Evolutionary Biology*, *17*, 133. https://doi.org/10.1186/s12862-017-0975-2

Raxworthy, C. J. (1988). A description and study of a new dwarf subspecies of smooth newt, *Triturus vulgaris*, from western Anatolia, Turkey. *Journal of Zoology*, *215*, 753–763.

Rohlf, F. J., & Corti, M. (2000). Use of two-block partial least-squares to study covariation in shape. *Systematic Biology*, *49*, 740–753. https://doi.org/10.1080/106351500750049806

Rohlf, F. J., & Slice, D. (1990). Extensions of the procrustes method for the optimal superimposition of landmarks. *Systematic Zoology*, *39*, 40–59. https://doi.org/10.2307/2992207

Sarkar, D. (2008). *Lattice: Multivariate data visualization with R*. Springer.

Sarkar, D., & Andrews, F. (2019). *LatticeExtra: Extra graphical utilities based on lattice* (version 0.6-29). R Package. https://CRAN.R-project.org/package=latticeExtra

Scholtes, S. J., Arntzen, J. W., Ajduković, M., & Ivanović, A. (2021). Variation in vertebrae shape across small-bodied newts reveals functional and developmental constraints acting upon the trunk region. *Journal of Anatomy*, *240*, 639–646. https://doi.org/10.1111/joa.13591

Shearman, R. M., & Burke, A. C. (2009). The lateral somitic frontier in ontogeny and phylogeny. *Journal of Experimental Zoology Part B: Molecular and Developmental Evolution*, *312*, 603–612. https://doi.org/10.1002/jez.b.21246

Slijepčević, M., Galis, F., Arntzen, J. W., & Ivanović, A. (2015). Homeotic transformations and number changes in the vertebral column of *Triturus* newts. *PeerJ*, *3*, e1397. https://doi.org/10.7717/peerj.1397

Toli, E. A., Bounas, A., Merilä, J., & Sotiropoulos, K. (2022). Genetic diversity and detection of candidate loci associated with alternative morphotypes in a tailed amphibian. *Biological Journal of the Linnean Society*, *137*, 465–474. https://doi.org/10.1093/biolinnean/blac103

Tourneville, A. (1879). Description d'une nouvelle espece de batracien urodèle d'espagne (Pelonectes boscai Lataste). Bulletin de la Société Zoologique de France, *4*, 69–87.

Urošević, A., Ajduković, M., Arntzen, J. W., & Ivanović, A. (2020). Morphological integration and serial homology: A case study of the cranium and anterior vertebrae in salamanders. *Journal of Zoological Systematics and Evolutionary Research*, *58*, 1206–1219. https://doi.org/10.1111/jzs.12374

Wagner, G. P., & Altenberg, L. (1996). Perspective: Complex adaptations and the evolution of evolvability. *Evolution*, *50*, 967–976. https://doi.org/10.1111/j.1558-5646.1996.tb02339.x

Wainwright, P. C. (2007). Functional versus morphological diversity in macroevolution. *Annual Review of Ecology, Evolution, and Systematics*, *38*, 381–401. https://doi.org/10.1146/annurev.ecolsys.38.091206.095706

Wellik, D. M. (2007). *Hox* patterning of the vertebrate axial skeleton. *Developmental Dynamics*, *236*, 2454–2463. https://doi.org/10.1002/dvdy.21286

Worthington, R. D., & Wake, D. B. (1972). Patterns of regional variation in the vertebral column of terrestrial salamanders. *Journal of Morphology*, *137*, 257–277. https://doi.org/10.1002/jmor.1051370302

Young, N. M., & Hallgrímsson, B. (2005). Serial homology and the evolution of mammalian limb covariation structure. *Evolution*, *59*, 2691–2704. https://doi.org/10.1111/j.0014-3820.2005.tb00980.x

Zelditch, M. L., & Goswami, A. (2021). What does modularity mean. *Evolution & Development*, *23*, 377–403. https://doi.org/10.1111/ede.12390

Zelditch, M. L., Swiderski, D. L., & Sheets, D. H. (2012). *Geometric morphometrics for biologists: A primer*. Elsevier Academic Press.

SUPPORTING INFORMATION

Additional supporting information can be found online in the Supporting Information section at the end of this article.

How to cite this article: Urošević, A., Ajduković, M., Vučić, T., Scholtes, S. J., Arntzen, J. W., & Ivanović, A. (2023). Regionalization and morphological integration in the vertebral column of Eurasian small-bodied newts (Salamandridae: *Lissotriton*). *Journal of Experimental Zoology Part B: Molecular and Developmental Evolution*, *340*, 403–413. https://doi.org/10.1002/jez.b.23205

APPENDIX A: ANALYZED MATERIAL WITH SCIENTIFIC NAME, TAXONOMIC AUTHORITY, SAMPLE SIZE (N), COLLECTION IDENTIFICATION NUMBERS (ID), LOCALITY OF ORIGIN, AND TYPE OF PRESERVATION (ETHANOL-PRESERVED WHOLE ANIMALS AND GLYCERIN-STORED SKELETONS).

Species and (sub)species	N	Collection	ID	Locality	Preservation
Lissotriton schmidtleri (Raxworthy, 1988)	13	IBISS	OZ 58 G21921; OZ 58 G21932; OZ 58 G21934; OZ 58 G2193235; OZ 58 G21937-40; OZ 58 G21948-50; OZ 58 G21952; OZ 58 G21953	Efes, Turkey	Glycerin
L. v. meridionalis (Boulenger, 1882)	8	IBISS	2373 15625; 2373 15629; 2373 15633; 2373 15641-44; 2373 15646	Podstrmec, Slovenia	Ethanol
L. v. ampelensis (Fuhn, 1951)	6	IBISS	OZ 62 G22595; OZ 62 G22598; OZ 62 G22600-03	Garda de Sus, Romania	Glycerin
L. v. vulgaris (Linnaeus, 1758)	5	IBISS	2579 17780; 2579 17788; 2579 17795; 2579 17797; 2579 17813	Valjevo, Serbia	Glycerin
L. v. vulgaris (Linnaeus, 1758)	20	ZMA.RENA	9270 (1–20)	Marcillé-la-Ville, France	Ethanol
L. v. vulgaris (Linnaeus, 1758)	22	RMNH.RENA	9521 (1–14); (G, H, J-M, O, P)	Hoensbroek, The Netherlands	Ethanol

Abbreviations: IBISS — University of Belgrade, Institute for Biological Research "Siniša Stanković" — National Institute of the Republic of Serbia; RMNH.RENA and ZMA.RENA — Naturalis Biodiversity Center, Leiden, The Netherlands.

APPENDIX B: THE CONFIGURATION OF 14 THREE-DIMENSIONAL LANDMARKS IDENTIFIED ON THE ATLAS AND 18 THREE-DIMENSIONAL LANDMARKS ON THE TRUNK AND SACRAL VERTEBRAE OF *LISSOTRITON* NEWTS (FOR A VISUALIZATION SEE FIGURE 1b).

Structures	Number	Description
Atlas	1	Tip of processus odontoideus
	2, 3	Maximal constriction of processus odontoideus
	4, 5	Most lateral point of occipital joint
	6, 7	Tip of the lamina
	8	Tip of the vertebra on the dorsal side
	9, 10	Maximal constriction of vertebra
	11, 12	Maximal curvature of the postzygapophysis
	13	The end of vertebra on the dorsal side
	14	Tip of the cotylus
Trunk and sacral vertebrae	1	Neural arch—anterior, above vertebral foramen
	2, 3	Prezygapophysae—anterolateral margins
	4, 6	Neural arch—lateral margin at the level of rib-bearers
	5, 7	Maximal constriction of the postzygapophysis
	8, 10	Parapophyses—articulation point
	9, 11	Diapophyses—articulation point
	12, 13	Postzygapophysae—posterio-lateral margins
	14	Neural spine—the most anterior part
	15	Neural spine—the middle part
	16	Neural spine—the most posterior part
	17	The anterior tip of the condylus
	18	Tip of the cotylus